

Engineering of Glasses for Advanced Optical Fiber Applications

Nathan Carlie, Laeticia Petit, Ph.D., Kathleen Richardson, Ph.D.

Clemson University School Of Material Science and Engineering/COMSET, Clemson, SC, USA

Correspondence:

Nathan Carlie, email: ncarlie@clemson.edu

ABSTRACT

Advanced optical applications (such as fiber optics) demand the engineering of innovative materials which provide the requisite optical performance in a form with specific functionality necessary for the desired application. We will report on recent efforts to engineer new non-oxide glasses with tailored photo-sensitive response, and multi-component oxide glasses optimized for use in next generation Raman amplification applications. The ultimate performance of such glasses relies on control of the formation and stability of defective and/or metastable structural configurations and their impact on physical as well as linear and nonlinear optical properties. Direct laser writing has drawn considerable attention since the development of femtosecond lasers and the recognition that such systems possess the requisite intensity to modify, reversibly or irreversibly the physical properties of optical materials. Such “structuring” has emerged as one of several possible routes for the fabrication of waveguides and other photo-induced structures.

INTRODUCTION

The demands for high-speed optical communications are increasing at a tremendous rate. In order to satisfy this need for information flow over short and long distance networks, a more efficient use of available communication channels is required. Along with the growing interest in these materials for optoelectronic and telecommunication applications comes a need to understand any modification or variation in their properties resulting from the transformation from bulk material to thin film form for planar waveguide writing using laser exposure or to fiber. There are three aspects to the development of new optical materials. First is the identification of glass compositions suitable for fiberization or planarization

and an understanding of the materials’ properties. Second is the fiber drawing or film deposition step followed by the fiber and film characterization. Third is the optimization of the composition for low optical loss, resistance to optical damage and strength.

In this paper, we present our study on the optimization of glass composition suitable for fiber drawing. The structure and luminescence properties between the bulk and the corresponding fiber are first compared. Then, we further explain how to tailor the composition of the glasses for high intensity and broad bandwidth Raman gain. Finally, we will present different target preparations to deposit chalcogenide and oxysulfide film and film response under laser exposure. We further propose and discuss structural mechanisms believed to be taking place upon laser exposure of these materials. Understanding the relationship between the optical properties and the response of the ChG under laser irradiation is a prerequisite toward the successful development of laser waveguide writing in these glasses.

ENGINEERING OF OXIDE GLASSES

Rare earth doped glasses, as laser materials for amplifiers at 1500 nm, have received much attention [1], as they offer significant application possibilities in the area of optical communications. Silica fibers and germanium-doped silica fibers have been deployed in optical communications systems as Raman gain media where the transmission fiber itself becomes the amplifying medium. The Raman amplifier can operate over the entire telecommunications window from 1250 to 1650 nm whereas, the Erbium amplifiers (EDFAs) are limited to a 100 nm band centered around a wavelength of 1550 nm.

Borophosphate Based Glasses for Amplification At 1550 nm

The successful development of optical amplifiers for long-distance communication systems has increased the interest in rare earth doped materials [2]. The possible integration of such systems in optical devices, correlated with the development of high power diode lasers used as a pump source, has opened the area of integrated optics. For such devices, high rare earth concentrations are necessary. The Er^{3+} ions have shown their potential for amplification around 1550 nm due to the possible excitation at 980 nm in the diode laser wavelength domain. Several investigations have mentioned that high linear index materials may exhibit interesting erbium luminescence such as a broadening of the spectrum and an increase of absorption and of excitation cross sections. In terms of light coupling in waveguide structure, they should also offer a wider optical aperture which is more practical.

For several years, phosphate matrices which include large amounts of d^0 ions have been studied [3]. Niobium oxide has been demonstrated to be highly polarizable and to be a more suitable d^0 metal ion for glass network formation. We have shown that large amounts of niobium oxide have been successfully incorporated in a borophosphate matrix [4]. These glasses have been elaborated by a standard melting method in a platinum crucible at 1000-1200°C for 1h under oxygen gas to prevent the reduction of Nb^{5+} . Long glass preforms, 1 cm in diameter and 8 cm in length, were formed by quenching in carbon molds that were preheated at the glass transition temperature (T_g). These preforms were then annealed for 15h at 30°C below T_g and finally used to draw mono-index fibers by pulling niobium glass rods on a fiber-drawing tower. At least 80 ft of fiber of 130 μm in diameter were formed by drawing at 3.5 m/min under a helium environment.

In order to compare the structure of the preform to the corresponding fiber, Raman spectroscopy has been performed. The Raman spectra are exhibited in *Figure 1*.

One can notice that identical Raman response has been obtained for the preform and the resulting fiber showing a similar glass network of the preform and of the fiber. The bands located at 820 cm^{-1} , 720 cm^{-1} and 650 cm^{-1} have been associated with corner-shared NbO_6 octahedra and the one at 680 cm^{-1} to the formation of a three dimensional NbO_6 network [3].

The absence of sharp peaks in the Raman spectra indicates the absence of crystallization in the fiber.

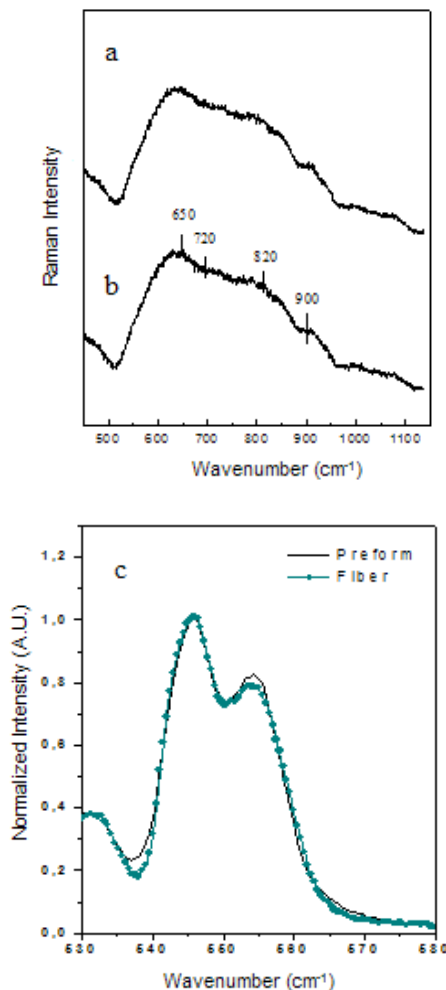


FIGURE 1. Raman spectra of Er^{3+} doped niobium borophosphate fiber (a) and preform (b). Visible emission spectra of Er^{3+} in the preform and in the fiber ($\lambda_{\text{exc}}=488\text{ nm}$) (c).

The visible emission spectra of the preform and fiber were measured at room temperature under 488 nm excitation, on bulk preform and fiber samples, shown in *Figure 1.c*. The emission spectra of the preform and the fiber exhibit a broad green luminescence with two maxima at 544 and 556 nm. This band has been assigned to the transition of the Er^{3+} ion from the $^4\text{S}_{3/2}$ excited level to the $^4\text{I}_{15/2}$ ground state. The absence of sharp peaks in the emission spectra of the fiber, as compared to the preform's response, provides further evidence that no crystallization around erbium ions, during the fiberization process of Er^{3+} doped niobium borophosphate glasses is occurring. The emission spectra are in agreement with the preservation of the

glassy structure without modification of the first coordination shell of erbium.

Tellurite and Borophosphate Based Glasses for Raman Gain Amplification

In our prior work [5-9] it has been shown that two families of glasses can be compositionally tailored and synthesized to form good optical quality candidate bulk glasses which possess either high spontaneous Raman intensity (which correlates with high Raman gain) or broad spectral bandwidth.

Borophosphate-Based Glasses for Broadband amplification

Because of their broad Raman bandwidth and flat-gain response over their usable bandwidth [6, 10] borophosphate glasses have also been extensively studied for the purpose of bandwidth optimization [6]. To increase the spectral breadth of the spontaneous Raman curves, multiple network formers whose vibrations spanned different regions have been combined. *Figure 2* shows the Raman spectra of some borophosphate glasses.

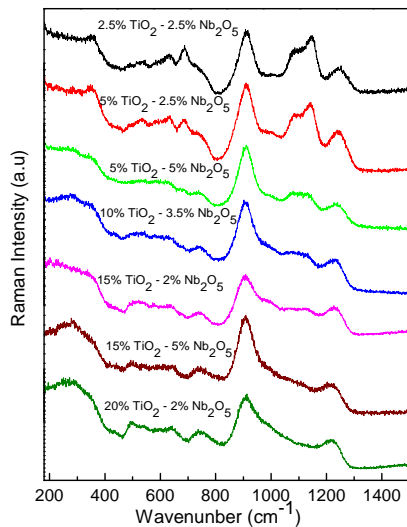


FIGURE 2. Raman spectra of [95%NaPO₃-5%Na₂B₄O₅] glass matrix with different TiO₂ – Nb₂O₅ molar ratios. (λ_{exc} = 632.8 nm)

The main Raman bands have been assigned to specific configurations of the network species and attributed to various phosphate vibrations. For instance, the band between 600 and 800 cm⁻¹ has been assigned to P-O-P symmetric stretch vibrations, while the peak at around 1080 cm⁻¹ corresponds to the antisymmetric P-O-P stretch of phosphate chains. The higher frequency peaks at 1145 cm⁻¹ and 1250 cm⁻¹ have been attributed to the ν_s -PO₂ and ν_{as} -PO₂ modes respectively [11]. Moreover, the Raman peak

near 910 cm⁻¹ is due to the superposition of Nb₂O₅ and TiO₂ Raman vibrations [12]. Note that changing the TiO₂ to Nb₂O₅ molar ratios changes the glass network structure. In addition, by comparing the different Raman spectra in *Figure 2*, one can see that the Nb₂O₅ Raman vibration appears to be stronger than the TiO₂ Raman vibration. The results of this study show that borophosphate glasses with d⁰ ions exhibit Raman vibrations up to 1300 cm⁻¹ (equivalent to almost 50 THz of bandwidth available for amplification).

Tellurite-Based Glasses for High Raman Gain Amplification

Tellurite glasses appear to be promising candidates for high gain/narrow bandwidth applications due to their high polarizability and nonlinear properties [6, 13-15]. A series of lead phospho-tellurite glasses were prepared to evaluate the impact of network former type (TeO₂ / P₂O₅ ratio) and the influence of other heavy metal oxide additives, such as PbO and Sb₂O₃.

The spontaneous Raman cross-section of the TeO₄ unit vibration, near 665 cm⁻¹ Raman band, referenced to known standards [16], has been calculated from the spontaneous Raman measurements to estimate the Raman gain coefficient [6]. The relative differential Raman cross-section and the estimated Raman gain coefficient are presented in *Figure 3 (a and b)*.

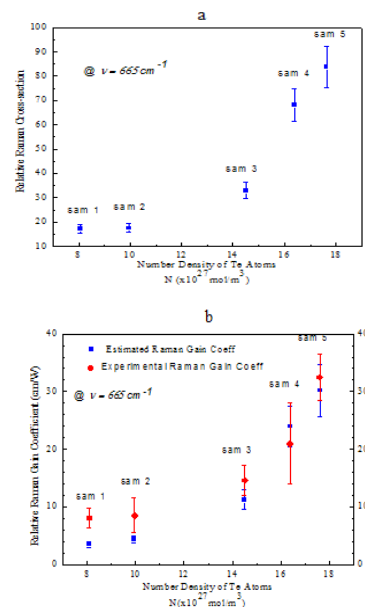


FIGURE 3. Variation of Raman cross-section (a) and Raman gain coefficient (b) at 665 cm⁻¹ relative to SiO₂. With sam 1 to 5: 48 TeO₂ – 17 PbO – 17 P₂O₅ – 18 Sb₂O₃, 56 TeO₂ – 20 PbO – 20 P₂O₅ – 4 Sb₂O₃, 76.5 TeO₂ – 9 PbO – 9 P₂O₅ – 5.5 Sb₂O₃, 85 TeO₂ – 10 Nb₂O₅ – 5 MgO and 85 TeO₂ – 15 WO₃

As predicted in the literature [17], the higher the TeO_2 concentration, the more TeO_4 units, and thus the higher the differential Raman cross-section and Raman gain coefficient values for the 665 cm^{-1} band as seen in this figure. Tellurite glasses exhibit Raman gain coefficients up to 30 times of that SiO_2 [7].

The exponential behavior of the spontaneous Raman cross-section data, and consequently the Raman gain coefficient, can be correlated to the fact that as the TeO_2 concentration increases, the relative amount of TeO_{3+1} and TeO_3 units inside the network structure decreases, consequently, the number of TeO_4 units has to increase. This leads to a strong and narrow peak at 665 cm^{-1} . One can notice that the estimated results for these glasses are in very good agreement (within $\pm 10\%$) with the previous experimental values obtained [7], within the errors of the theoretical and experimental predictions. This shows it is possible to predict the Raman gain of glasses based on knowledge/measurement of the scattering cross-section of the dominant network species.

ENGINEERING OF CHALCOGENIDE GLASSES

The Glass Processing and Characterization Laboratory (GPCL) at Clemson University is also well known for their work in Chalcogenide glasses (ChG's) [18-23]. ChG's are based on the chalcogen elements S, Se, and Te, and the addition of other elements such as Ge, As, and Sb can lead to the formation of stable glasses [24]. Previous works have reported that sulfide glasses show higher nonlinear optical properties than oxide glasses [25-27]. ChG's have drawn great attention recently due to their potential as candidates for applications in infrared optics and photonics devices [28]. These materials possess several key advantages compared to the corresponding oxide glasses, including excellent infrared transparency, high refractive index, and wide variations of the refractive index depending on their chemical composition [29]. Cerqua-Richardson et al. have compared the nonlinear optical properties of these chalcogenide glasses in both bulk and thin-film form [18].

Sulfide Based Films

The GPCL group has developed the processing techniques necessary for the fabrication of reproducible and homogenous ChG optical materials. This research has focused mainly on the general study of glasses in the As-S-Se system and specifically the compositions As_2S_3 and As-S-Se [19, 20, 30] as As_2S_3 glasses have been shown to have a nonlinear Kerr effect 80 times larger than fused silica

[31]. Moreover, their ability to be integrated into fiber and film-based devices has been demonstrated [32]. These glasses were prepared from high purity elements using a standard melting method. Starting materials were weighed and batched inside a nitrogen-purged glove box and sealed using a gas-oxygen torch under vacuum into quartz ampoules. Prior to sealing and melting, the ampoule and batch were pre-heated at 110°C for 4 h to remove surface moisture from the quartz ampoule and the batch raw materials. The ampoule was then sealed and heated for 24 hours at different temperatures, depending on the glass composition. Once homogenized using a rocking furnace, the melt-containing ampoule was air-quenched to room temperature. To avoid a fracture of the tube and glass ingot, the ampoules were subsequently returned to the furnace for annealing for 15 hours at 40°C below the glass transition temperature, T_g .

Nonlinear optical properties of As-S-Se chalcogenide glasses were measured by the Z-scan technique at 1600 nm. The nonlinear refractive indices (n_2) of the glasses are listed in the table below:

TABLE I. Linear and nonlinear refractive indices (relative to silica) for bulk glasses in the As-S-Se system

Linear and non-linear refractive indices of glasses at 1.6 μm			
Glass number	Glass composition	Linear index n_0 (± 0.01)	Non-linear index n_2 (glass)/ n_2 (SiO_2) ($\pm 10\%$)
	SiO_2	1.45	1
1	As_2S_3	2.38	73
2	$\text{As}_{40}\text{S}_{15}\text{Se}_{45}$	2.48	77
3	$\text{As}_{40}\text{S}_{30}\text{Se}_{30}$	2.60	105
4	$\text{As}_{40}\text{S}_{45}\text{Se}_{15}$	2.70	190
5	$\text{As}_{40}\text{Se}_{60}$	2.80	295
7	$\text{As}_{24}\text{S}_{38}\text{Se}_{38}$	2.45	406

It is shown in *Table I*, that the introduction of selenium to the As-S glass system increases n_2 up to 400 times the n_2 for silica. We have correlated such a large n_2 for glasses with small As/(S+Se) molar ratios to the presence of covalent, homopolar Se-Se bonds in the glass structure [20].

These glasses have been used as targets for film deposition using the thermal evaporation technique. *Figure 4* exhibits the Raman spectra of the bulk glasses used as targets and of the corresponding films.

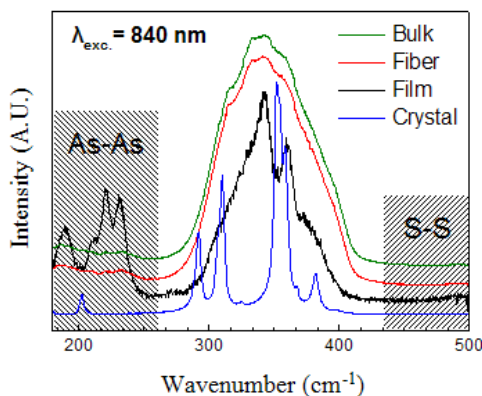


FIGURE 4. Raman spectra obtained at 840 nm excitation for As_2S_3 bulk glass, optical fiber, thin film and crystal.

The spectra exhibit two bands: one between 200 and 280 cm^{-1} , and the other between 300 and 400 cm^{-1} . The band at higher wavenumber has been attributed to the As-S-As antisymmetric stretch, while the lower energy bands correspond to the vibrations of As-As or S-S homopolar bonds [20]. Compared to the bulk glass, the film shows a narrowing of the main band around 330 cm^{-1} , the formation of a shoulder near 365 cm^{-1} , and an increase of the intensity of the bands from 200 to 250 cm^{-1} . These modifications indicate differences in the network structure between bulk and their corresponding films; specifically, the existence of metastable and photo-sensitive homopolar As-As and S-S bonds [20].

As_2S_3 film has been irradiated using visible cw and IR fs laser exposure. After laser exposure, we noticed that i) the film photo-expanded and ii) the photo-expansion increased up to 150 nm with an increase of the laser power when irradiated at 514 nm and up to 35 nm when irradiated at 785 nm. The difference in photo-expansion has to be related to the irradiation wavelength which induces one or multi-photon absorption when irradiated at 514 or 785 nm respectively. Figures 5.a and b present, respectively, a nearfield output of a 2 cm long As_2S_3 planar waveguide written using 514 nm argon laser after 20 s exposure, and using an extended cavity Ti:sapphire laser with a 40 nm spectral bandwidth centered at 800 nm, which produced 20 nJ pulses of 30 fs duration at a repetition rate of 25 MHz.

The structural modification of the film has been studied using Raman spectroscopy. Figure 6 exhibits the Raman spectra of As_2S_3 films before and after irradiation. The Raman spectrum of the film after irradiation exhibits a slight decrease of the shoulder at 365 cm^{-1} and an increase of the bands located in the range 200 to 250 cm^{-1} . This indicates a change in

the glass network with the creation of homopolar bonds As-As and S-S after laser irradiation.

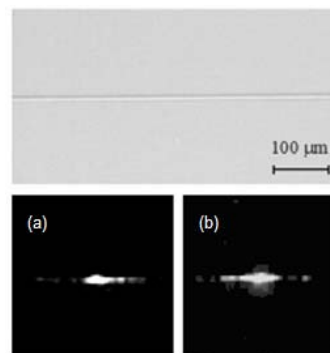


FIGURE 5. Micrograph of a typical waveguide and the far-field output of waveguides written by 514 nm CW (a) and 800 nm femtosecond (b) laser irradiation.

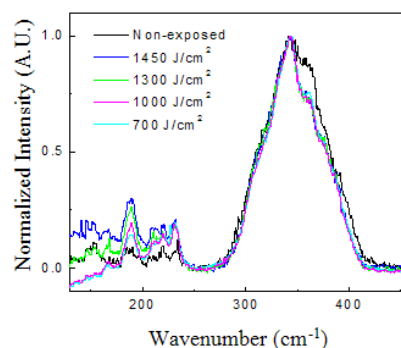


FIGURE 6. Raman spectra of As_2S_3 thin film before and after 800 nm femtosecond irradiation ($\lambda_{\text{exc}} = 840 \text{ nm}$)

Similar work has been done on Ge-Ga-Sb-S-Se glass systems. We have developed glasses in the Ge-Sb-S system with low Sb concentrations and with an excess of S which exhibit good physical stability and a high nonlinear index suitable for use in novel optical applications. In order to increase the nonlinear refractive index in accordance with the study of As-S-Se glass system, Sulfur has been replaced progressively by Selenium. To create a matrix amenable to rare earth doping in the germanate glass network, a limited fraction of Ge has been replaced by Ga. In this context, glasses in the Ge-Ga-Sb-S-Se glass host system have been prepared and characterized for their physical and optical behavior [33]. The n_2 of these germanium-based chalcogenide glasses have been measured using a modified Z-Scan technique with picosecond pulses emitted by a 10 Hz Q-switched mode-locked Nd-Yag laser at 1064 nm under conditions suitable to characterize ultrafast nonlinearities. We have shown that n_2 depends on the glass composition and hence, on the structure of the glass [22, 23].

TABLE II: Nonlinear refractive index and two-photon absorption coefficients at 1064 nm for the Ge-Ga-Sb-S-Se system

Glass Composition	n_2 ($10^{-18} \text{ m}^2/\text{W}$)	n_2/n_{silica}	Total Electronic Lone Pairs	β (cm/GW)	λ_{gap} (nm)	F
CS_2^9	3			—		
$90\text{GeS}_2-10\text{Sb}_2\text{S}_3$	1.84	61	5.3×10^{22}	0.15	529	1.7
$85\text{GeS}_2-15\text{Sb}_2\text{S}_3$	1.9	63	5.34×10^{22}	<0.1	571	<1.1
$60\text{GeS}_2-40\text{Sb}_2\text{S}_3$	7.42	246	5.69×10^{22}	1.17	705	3.3
$\text{Ge}_{23}\text{Sb}_7\text{S}_{70}$	1.66	55	5.44×10^{22}	<0.1	532	<1.1
$\text{Ge}_{23}\text{Sb}_{12}\text{S}_{65}$	2	67	5.97×10^{22}	<0.1	612	<1.1
$\text{Ge}_{23}\text{Sb}_7\text{S}_{60}\text{Se}_{10}$	1.93	64	5.51×10^{22}	<0.1	643	<1.1
$\text{Ge}_{18}\text{Ga}_5\text{Sb}_7\text{S}_{70}$	1.96	65	1.24×10^{23}	<0.1	578	<1.1

Shown in *Table II*, the nonlinear index increases significantly up to 246 times the n_2 for fused silica with an increase of SbS_3 units and also very slightly with the replacement of Ge by Ga or S by Se. We have attributed the variation of n_2 to the total number of electronic lone pairs and to the position of the absorption band gap which are induced by the presence of GaS_4 units or of covalent and homopolar Se-Se bonds in the glass structure [22].

We have observed that these glasses are also sensitive to IR femtosecond laser exposure and exhibit a structural photo-expansion of the sample surface after laser irradiation. We have shown that: i) the photo-sensitivity of the glass as well as the magnitude of photo-expansion depends on glass composition ii) through spectroscopic examination, that this photo-response may be related to structural changes [33]. It is interesting to point out that the changes in structure are quite different to those observed for the As-S-Se system. In this glass network, the property changes arise due to changes in interconnections between GeS_4 units, rather than homopolar bond formation.

It can be seen that the use of photo-exposure of chalcogenide materials is a very attractive method for the processing of planar optical devices. Additionally, the ability to translate the material in three dimensions during femtosecond irradiation allows the formation of volumetric refractive index changes which is very promising for the development of devices in bulk materials, such as, all-optical circuits.

Oxysulfide Based Film

Because of the photo-sensitivity of chalcogenide based glasses which lead to structural modification as seen in the previous paragraph, oxysulfide glasses have been developed for optical applications as it has been shown that these new glasses should offer the possibility of combining the mechanical properties of oxide materials with the attractive optical traits of

sulfide glasses by adjusting the sulfur to oxygen ratio [34, 35]. Moreover, Sulfur plays an important role in the nonlinear optical properties in oxysulfide glasses because of their large atomic radius. This effect was recently demonstrated by Zhou et al. who showed that the substitution of oxygen anions with sulfur anions increases by one order of magnitude the $\chi^{(3)}$ [36]. These glasses have been reported to exhibit better chemical stability and to be more resistant to atmospheric attack in comparison with the corresponding sulfide glasses [34].

Our previous study demonstrated the successful production of amorphous oxysulfide materials through the sulfination of different starting oxide materials [21]. Oxysulfide glasses were prepared by surface sulfination of glass samples by heating to different temperatures under H_2S flow for a few hours. It is possible to control the O/S ratio, checked using Energy Dispersive Spectroscopy (EDS), by changing the temperature and the duration of the sulfination heat treatment. *Figure 7* below is the Raman spectrum of crystallized GeO_2 before and after complete sulfination heat treatment at 550°C for 24 hours.

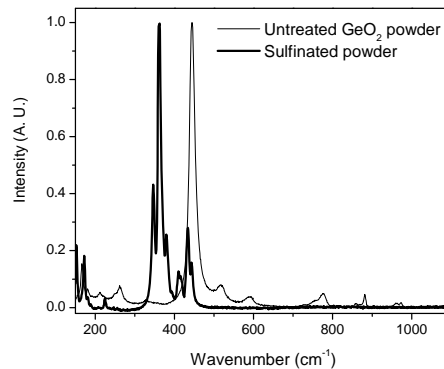


FIGURE 7. Raman spectrum of crystallized GeO_2 before and after sulfination heat treatment ($\lambda_{\text{exc}} = 632 \text{ nm}$)

The spectra show that the main peak shifts from 444 cm^{-1} which corresponds to Ge-O bonds to 360 cm^{-1} corresponding to Ge-S bonds.

Thin germanium based oxysulfide films were deposited onto glass substrates by RF sputtering under low pressure argon atmosphere from a “home prepared” target, obtained from pressing oxysulfide powder into discs. These targets were prepared by pressing 15 g of sulfinated powder into 5 cm pellets which were annealed at 200°C for 15 hours. The composition of the film was found to be $\text{GeO}_{1.65}\text{S}_{0.35}$ using EDS. *Figure 8* presents the Raman spectra of this film.

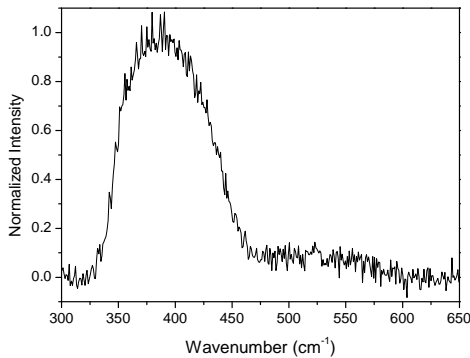


FIGURE 8. Micro-Raman spectrum of the oxysulfide film ($\lambda_{\text{exc}} = 632.8 \text{ nm}$)

The main Raman band of the deposited GeOS films is observed at 390 cm^{-1} . This band is centered between the main bands of GeO_2 and GeS_2 . This fact, along with the width of this band, suggests the possible formation of homogeneous amorphous oxysulfide material, rather than a simple mixture of the oxide and sulfide as a summation of the pure sulfide and oxide spectra cannot describe this band. It was found that the films possessed optical inhomogeneities in the form of multiple layers within the film. These inhomogeneities were in fact due to the formation a secondary layer of lower index within the film with an approximate thickness between 50 nm and 200 nm.

Photo-sensitivity of the film has been tested using a high intensity laser irradiation at 480 nm, generated by a frequency tripled Nd:YAG laser equipped with an OPO at a pulse rate of 10 Hz. After laser exposure, a change in the interference pattern as well as a red shift in the absorption edge toward longer wavelengths have been observed as seen in *Figure 9* below.

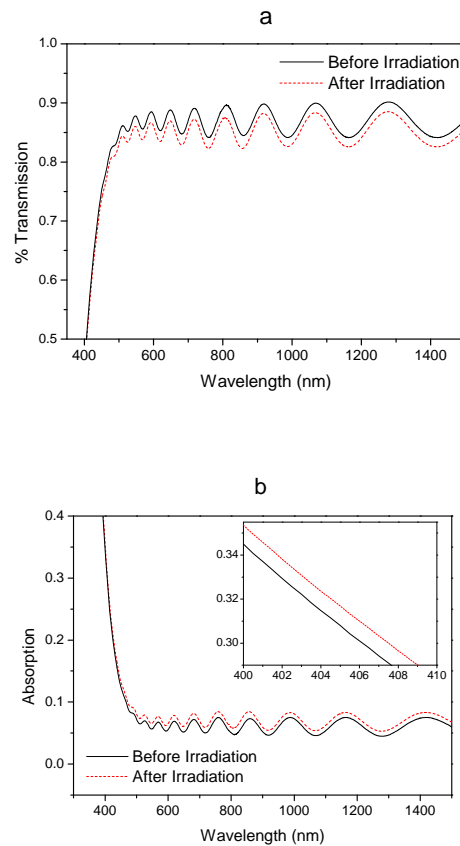


FIGURE 9. Transmission (a) and absorbance (b) spectra of the oxysulfide film before and after irradiation

It was found that a change in the interference pattern indicates a change in the refractive index in the oxysulfide layer confirming that the oxysulfide glasses are also photo-sensitive to laser exposure.

CONCLUSION

In this paper, we have shown that we are able to optimize the composition of oxide, oxysulfide and chalcogenide glasses depending on the desired application. Tellurite and borophosphate glass network former-based compositions appear to be attractive candidates for Raman gain application purposes. The tellurite glasses exhibit an absolute Raman gain coefficient of up to 30 times higher than silica and borophosphate glasses with d^0 ions exhibit Raman vibration up to 1300 cm^{-1} . The intermediate and modifier glass constituents influence the glass network and the overall Raman gain performance of the glass. Borophosphate glass networks also appear to be a good host for rare earth ions and can be drawn into fiber with a similar structure and luminescence properties to the preform.

Chalcogenide based materials possess high nonlinear refractive indices which increase with an increase of Se content up to 400 times the n_2 of fused silica for $As_{24}S_{38}Se_{38}$ glass. These glasses can be successfully deposited into films using the thermal evaporation technique. Waveguides can be written in the surface using IR fs laser irradiation inducing a change of the linear refractive index. This has been attributed to different mechanisms: creation of As-As and S-S bonds in As-based glasses and to changes in interconnections between GeS_4 units in Ge-based glasses.

Finally, we have shown that oxysulfide films, deposited from a sulfinated target using RF sputtering technique, are also sensitive to laser exposure with a change of the refractive index and a red-shift of the absorption band gap. Such modification opens the pathway toward the laser writing of photonic devices in the surface of the chalcogenide and oxysulfide materials.

ACKNOWLEDGEMENTS

The authors would like to thank students who have participated in these studies: C. Rivero, C. Lopez, A. Zoubir, T. Anderson, and J. Choi. The authors further thank their collaborators at the University of Central Florida, in Florida/US, the Universities of Angers, Limoges and of Bordeaux/ France, as well as the University of Laval in Quebec/Canada for their contributions to this research over the years. Finally we acknowledge the National Science Foundation for their support ECS-0225930, ECS- 0123484, INT-0129235, DMR-9912975, DMR-0312081, DMR-0321110, EEC-0244109, & NSF/CNRS # 13050

REFERENCES

1. Kinoshita, S., T. Okiyama, and K. Moriya, *Sci. Tech. J.*, Vol. 35, 1999, pp. 82-85
2. Miniscalco, W.J., *J. Lightwave Tech.*, Vol. 9, 1991, pp. 243-250
3. Cardinal, T., E. Fargin, G. Le Flem, M. Couzi, L. Canioni, P. Segonds, L. Sarger, A. Ducasse, and F. Adamietz, *J. Solid State Inorg. Chem.*, Vol. 33, 1996, pp. 597-605
4. Petit, L., T. Cardinal, J.J. Videau, Y. Guyot, M. Boulon, M. Couzi, and T. Buffeteau, *J. Non-Cryst. Solids*, Vol. 351, 2005, pp. 2076-2084
5. Rivero, C., K. Richardson, K. Stegeman, G. Stegeman, T. Cardinal, E. Fargin, and M. Couzi, *Glass Technol.*, Vol. 46, 2005, pp. 80-84
6. Rivero, C., K. Richardson, R. Stegeman, G. Stegeman, T. Cardinal, E. Fargin, M. Couzi, and V. Rodriguez, *J. Non-Cryst. Solids*, Vol. 345&346, 2004, pp. 396-401
7. Stegeman, R., L. Jankovic, H. Kim, C. Rivero, G. Stegeman, K. Richardson, P. Delfyett, A. Schulte, Y. Guo, and T. Cardinal, *Optics Letters*, Vol. 28, 2003, pp. 1126-1128

8. Stegeman, R., C. Rivero, G. Stegeman, K. Richardson, P. Delfyett, L. Jankovic, and H. Kim, *J. Opt. Soc. B.*, Vol. 22, 2005, pp. 1861-1867
9. Stegeman, R., C. Rivero, K. Richardson, G. Stegeman, P. Delfyett, Y. Guo, A. Pope, A. Schulte, T. Cardinal, P. Thomas, and J. Champarnaud-Mesjard, *Optics Express*, Vol. 13, 2005, pp. 1144-1149
10. Dianov, E.M., M.V. Grekov, I.A. Bufetov, S.A. Vasiliev, O.I. Medvedkov, P.V. G., V.V. Koltashev, A.V. Belov, M.M. Bubnov, S.L. Semjonov, and A.M. Prokhorov, *Electron. Lett.*, Vol. 33, 1997, pp. 1542-1544
11. Rulmont, A., R. Cahay, M. Liegeois-Duckaerts, and P. Tarte, *Eur. J. Solid State Inorg. Chem.*, Vol. 28, 1991, pp. 207-219
12. Ayyub, P., M.S. Multani, V.R. Palkar, and R. Vijayaraghavan, *Phys. Rev. B*, Vol. 34, 1986, pp. 8137-8140
13. O'Donnel, M.D., K. Richardson, R. Stolen, C. Rivero, T. Cardinal, D. Furniss, and A.B. Seddon, *Opt. Mater.*, Vol. 30, No. 6, 2008, pp. 946-951
14. Rivero, C., R. Stegeman, K. Richardson, G. Stegeman, G. Turri, M. Bass, P. Thomas, M. Udovic, T. Cardinal, E. Fargin, M. Couzi, H. Jain, and A. Miller, *J. Appl. Phys.*, Vol. 101, No. 2, 2007,
15. O'Donnel, M.D., A.B. Seddon, D. Furniss, C. Rivero, M. Ramme, R. Stegeman, G. Stegeman, K. Richardson, R. Stolen, M. Couzi, and T. Cardinal, *J. Am. Ceram. Soc.*, Vol. 90, No. 5, 2007, pp. 1448-1457
16. Pan, Z., H. Morgan, and L.B. H., *J. Non-Cryst. Solids*, Vol. 185, 1995, pp. 127-134
17. Fargin, E., A. Berthereau, T. Cardinal, G. Le Flem, L. Ducasse, L. Canioni, P. Segonds, L. Sarger, and A. Ducasse, *J. Non-Cryst. Solids*, Vol. 203, 1996, pp. 96-101
18. Cerqua-Richardson, K.A., J.M. McKinley, L. B., and A. Villeneuve, *Opt. Mater.*, Vol. 10, 1998, pp. 155-159
19. Viens, J., C. Meneghini, A. Villeneuve, T. Galstian, E. Knystautas, M. Duguay, K. Richardson, and T. Cardinal, *J. Lightwave Technol.*, Vol. 17, No. 7, 1999, pp. 1184-1191
20. Cardinal, T., K.A. Richardson, H. Shim, A. Schulte, R. Beatty, K. Le Foulgoc, C. Meneghini, J.-F. Viens, and A. Villeneuve, *J. Non-Cryst. Solids*, Vol. 256&257, 1999, pp. 353-360
21. Petit, L., K. Richardson, B. Campbell, G. Orvellion, T. Cardinal, F. Guillen, C. Labrugere, P. Vinatier, M. Couzi, W. Li, and S. Seal, *Phys. Chem. Glasses*, Vol. 45, 2004, pp. 315-322
22. Petit, L., N. Carlie, T. Anderson, M. Couzi, J. Choi, M. Richardson, and K.C. Richardson, *Optical Materials*, Vol. 29, 2007, pp. 1075-1083
23. Petit, L., N. Carlie, A. Humeau, G. Boudebs, H. Jain, A.C. Miller, and K. Richardson, *Mat. Res. Bull.*, Vol. 42, No. 12, 2007, pp. 2107-2116
24. Sanghera, J.S., L.B. Shaw, and I.D. Aggarwal, *C. R. Chimie.*, Vol. 5, 2002, pp. 873-878
25. Vogel, E.M., M.J. Weber, and D.M. Krol, *Phys. Chem. Glasses*, Vol. 32, 1991,
26. Nasu, H., Y. Ibara, and R. Kubodera, *J. Non-Cryst. Solids*, Vol. 110, 1989, pp. 229-234
27. Nasu, H., R. Kubodera, M. Kobayasi, M. Nakamura, and K. Kamiya, *J. Am. Ceram. Soc.*, Vol. 73, No. 1794-1796, 1990,
28. Ling, Z., H. Ling, and Z. Chengshan, *J. Non-Cryst. Solids*, Vol. 184, 1995, pp. 1-4
29. Seddon, A.B., *J. Non-Cryst. Solids*, Vol. 184, 1995, pp. 44-50

30. Li, W., S. Seal, C. Rivero, C. Lopez, K. Richardson, A. Pope, A. Schulte, S. Myneni, H. Jain, and K.M. Antoine, A. C., *J. Appl. Phys.*, Vol. 98, 2005, pp. 053503
31. Hall, D.W., M.A. Newhouse, N.F. Borelli, W.H. Dumbaugh, and D.L. Weidman, *Appl. Phys. Lett.*, Vol. 54, 1989, pp. 1293-1295
32. Asobe, M., T. Ohara, T. Kaino, and I. Yokohama, *Electron. Lett.*, Vol. 32, 1996, pp. 1396-1397
33. Petit, L., N. Carlie, R. Villeneuve, J. Massera, M. Couzi, A. Humeau, G. Boudebs, and K. Richardson, *J. Non-Cryst. Solids*, Vol. 352, No. 50-51, 2006, pp. 5413-5420
34. Kumta, P.M. and S.H. Risbud, *Ceram. Bull.*, Vol. 69, 1990, pp. 1977-1981
35. Maurel, C., T. Cardinal, P. Vinatier, L. Petit, K. Richardson, N. Carlie, F. Guillen, M. Lahaye, M. Couzi, F. Adamietz, V. Rodriguez, F. Lagugne-Labarhet, V. Nazabal, A. Royon, and L. Canioni, *Mat. Res. Bull.*, Vol. 43, No. 5, 2008, pp. 1179-1187
36. Zhou, Z.H., H. Nasu, T. Hashimoto, and K. Kamiya, *J. Mat. Res.*, Vol. 14, 1999, pp. 330-337

AUTHORS ADDRESSES

Nathan Carlie, Laeticia Petit, Ph.D., Kathleen Richardson, Ph.D.

Clemson University School of Materials Science and Engineering / COMSET
 161 Siring Hall
 Clemson University
 Clemson, SC 29630
 UNITED STATES